Solar Physics
DOI: 10.1007/•••••-•••-•••-••••-•

STEREO-A and PROBA2 Quadrature Observations of Reflections of three EUV Waves from a Coronal Hole

I.W. Kienreich[1] · **N. Muhr**[1, 2] ·
A.M. Veronig[1] · **D. Berghmans**[3] ·
M. Temmer[1] · **B. Vršnak**[2] · **D. Seaton**[3] ·

Abstract We investigate three consecutive large-scale coronal waves at the same coronal hole, simultaneously observed by the Solar TErrestrial Relations Observatory (STEREO)-A spacecraft and the PRoject for On-Board Autonomy 2 (PROBA2) spacecraft on January 27, 2011. All extreme-ultraviolet (EUV) waves originated from the same active region NOAA 11149 positioned at N30E15 in the STEREO-A field-of-view and precisely on the limb in PROBA2. The EUV waves were accompanied by coronal mass ejections (CMEs) and GOES class B/C flares. The propagation of the primary waves was directed southward with an angular extent of $\sim 120^\circ$ as seen from STEREO-A. We derive for the three primary EUV waves start velocities in the range of ~ 310 km/s up to ~ 500 km/s. Each large-scale wave was reflected at the boarder of the extended coronal hole at the southern polar region. The signatures of the reflected waves could be followed on-disk by STEREO-A as well as on the limb by PROBA2. The kinematical study of the reflected waves revealed that they were slower than their associated direct waves, having start velocities in the range of ~ 130 to 230 km/s, and that they experienced a distinct deceleration. The EUV wave reflections implicate that the EUV transients are indeed MHD waves.

Keywords: Shock waves, Coronal Mass Ejections

[1] Kanzelhöhe Observatory/IGAM,Institute of Physics, University of Graz, Universitätsplatz 5, A-8010 Graz, Austria email: ines.kienreich@uni-graz.at email: nicole.muhr@uni-graz.at email: asv@igam.uni-graz.at email: manuela.temmer@uni-graz.at
[2] Hvar Observatory, Faculty of Geodesy, Kačićeva 26, 1000 Zagreb, Croatia email: bvrsnak@gmail.com
[2] Royal Observatory of Belgium, Solar Physics, Ringlaan 3, B-1180 Brussels, Belgium email: david.berghmans@oma.be

1. Introduction

Large-scale disturbances propagating through the solar corona have been first imaged by the Extreme-Ultraviolet Imaging Telescope (EIT) onboard the Solar and Heliospheric Observatory (SOHO) about 15 years ago (e.g. Moses *et al.*, 1997; Thompson *et al.*, 1998). Since these days large-scale coronal waves, which have to become known as 'EIT waves' but are now more generally called extreme ultraviolet (EUV) waves, were frequently observed in the EUV wavelength range, which led to a large number of case studies (e.g. Thompson *et al.*, 1998; Wills-Davey and Thompson, 1999; Delannée and Aulanier, 1999; Warmuth *et al.*, 2001; Zhukov and Auchère, 2004; Podladchikova and Berghmans, 2005) and several statistical studies (Klassen *et al.*, 2000; Biesecker *et al.*, 2002; Thompson and Myers, 2009). Similar large-scale coronal transients were also detected in other wavelengths such as soft X-rays (e.g. Khan and Aurass, 2002; Hudson *et al.*, 2003; Vršnak *et al.*, 2006), microwaves (White and Thompson, 2005), and the metric domain (Vršnak *et al.*, 2006).

The investigations of large-scale coronal waves, however, were limited by the low imaging cadence of EIT ($\sim$ 12 min), resulting in a drastic undersampling particularly of fast events, where at most one single EUV wave front was recorded during such fast propagation. The launch of the Solar Terrestrial Relations Observatory (STEREO; Kaiser *et al.*, 2008) twin-spacecraft with its Extreme Ultraviolet Imager (EUVI) started a new era in high-cadence observations of the solar corona. Since more than four years it supplies observations of EUV waves with high time cadence from two different vantage points and over a large field-of-view up to 1.7 solar radii, providing us with new insights into the generation, evolution and 3D structure of large-scale EUV waves (e.g. Patsourakos and Vourlidas, 2009; Veronig *et al.*, 2010; Temmer *et al.*, 2011). Yet, albeit more than 15 years of continuous studies of EUV wave events, the nature and generation mechanism of EUV waves is still very controversially discussed. Most commonly they are interpreted as fast-mode magnetosonic waves, driven by the CME expansion and/or the explosive flare energy release (e.g. Wills-Davey, DeForest, and Stenflo, 2007; Patsourakos and Vourlidas, 2009; Veronig *et al.*, 2010). Some authors assume that these features are no waves at all and suggest they are related to a magnetic field line reconfiguration during the associated CME eruption, causing Joule heating or flare-like brightenings at the CME front (e.g. Delannée and Aulanier, 1999; Chen *et al.*, 2002; Attrill *et al.*, 2007; Dai *et al.*, 2010). In the last years also hybrid models combining both interpretations were developed (e.g. Cohen *et al.*, 2009; Liu *et al.*, 2010). For further discussion on the observational characteristics and models of EUV waves we refer to the recent reviews of Wills-Davey and Attrill (2010), Gallagher and Long (2010), Warmuth (2010), and Zhukov (2011).

Observations of interactions of large-scale EUV waves with active regions and coronal holes have been occasionally reported since the early days of SOHO. One of the first reports was given by Thompson *et al.* (1998) mentioning the halt of EUV waves at the border of coronal holes (CHs). Veronig *et al.* (2006) observed a partial penetration of Moreton waves into the realm of the coronal hole moving perpendicular to the CH border. A number of authors have found that EUV

waves were stopped or deflected from active regions (ARs); (e.g. Thompson *et al.*, 1999; Delannée and Aulanier, 1999; Chen and Fang, 2005). Others reported EUV waves moving along the outlines of active regions and coronal holes (Gopalswamy *et al.*, 2009; Kienreich *et al.*, 2011). Simulations treating the EUV waves as fast-mode magnetosonic waves supported these findings, as the model MHD waves underwent strong reflections at the borders of high Alfvén velocity areas, such as AR's and CH's (e.g. Wang, 2000; Ofman and Thompson, 2002).

The most intriguing and thus well studied EUV wave reflection was recorded on May 19, 2007 by the STEREO/EUVI instruments. Several papers report a strong reflection and refraction of an EUV wave disturbance at a coronal hole (e.g. Long *et al.*, 2008; Veronig, Temmer, and Vršnak, 2008). Gopalswamy *et al.* (2009) performed a detailed analysis of this event stating the occurrence of reflections at three different coronal holes. A contradictory study by Attrill (2010), however, questioned the wave reflections on May 19, 2007, arguing that the detected features were just artifacts in the running difference images, which were misinterpreted as reflected waves. Instead Attrill (2010) favored the interpretation that a two-part filament eruption had caused the onset of two EUV waves with the southward propagating wave experiencing a distinct rotation consistent with helicity of the associated CME. Hence, it is still a controverse matter, whether genuine EUV wave reflections have been observed so far, or, as Attrill (2010) assumed, whether they are just optical illusions, since in many cases EUV waves disappear or become 'stationary' at CH borders.

In this paper we present the first study of three large-scale EUV waves observed in quadrature, which were reflected of a coronal hole. We combine simultaneous STEREO-A on-disk observations, recording both the primary and reflected wave fronts, with the PRoject for On-Board Autonomy 2 (PROBA2; Berghmans *et al.*, 2006) spacecraft plane-of-sky observations of the wave propagation along the limb. This gives us the opportunity to compare the threedimensional structure of the primary and the reflected wave and to study the change in propagation height caused by the reflection process. Our main focus, however, lies on the kinematical analysis of the on-disk signatures of the reflected waves in relation to the kinematics of their primary counterparts.

2. Data and Methods

For the analysis of the EUV wave events under study, occurring on 2011 January 27, we use data from the STEREO/EUVI instrument, which is part of the Sun Earth Connection Coronal and Heliospheric Investigation (SECCHI; Howard *et al.*, 2008) instrument suite. Simultaneously we analyzed the waves' evolution in full-disk images by the Sun Watcher using Active Pixel system detector and image processing (SWAP; Halain *et al.*, 2010) on board the PROBA2 spacecraft. On January 27, 2011 STEREO/EUVI-A (henceforth ST-A) and SWAP were nearly in quadrature, i.e. $\sim 90^\circ$ apart. Accordingly, while ST-A recorded the EUV waves' on-disk evolution, SWAP observed their propagation along the solar limb. In our study we could only make use of the high-cadence STEREO/EUVI imagery in 195 Å (cadence: 5 min), since in 171 Å and 284 Å the cadence was

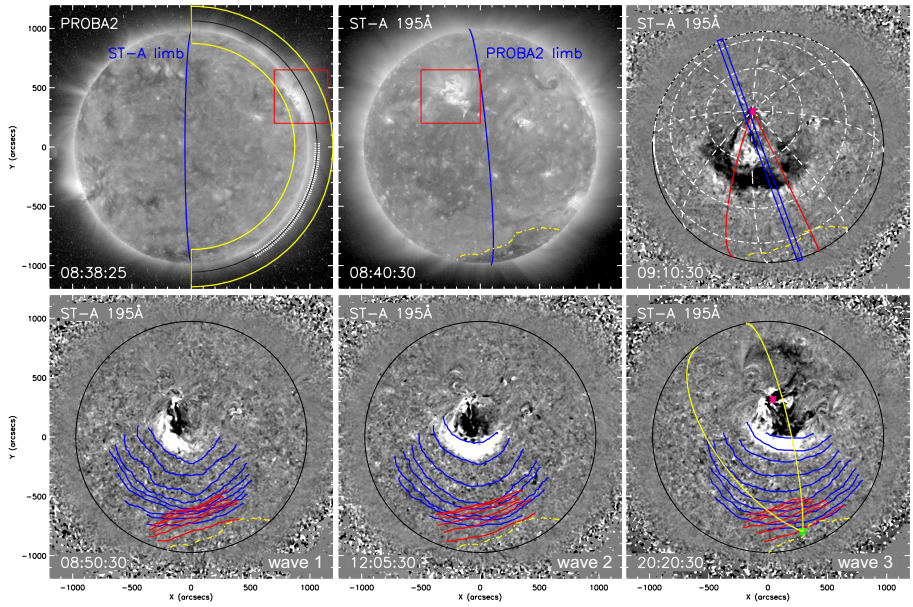

Figure 1. (a) PROBA2, (b) ST-A direct images indicating the position of the wave center within Active Region NOAA 11149 (red square) at the limb and on-disk,respectively. (a) Yellow semi-circles mark the region, for which off-limb stack-plots (cf. Fig. 5(a)-(b) and Fig. 6) were derived. (c)-(f) Median-filtered 10 minutes ST-A 195 Å running ratio (RR) images plus outlines of the southern coronal hole (yellow dash-dotted line) observed on 2011 January 27. (c) Red meridians give the delimiting 45° sector for the calculation of the primary waves' kinematics. The slices for the on-disk stack-plots of Fig. 5.(c)-(d) are represented by the blue rectangle. (d)-(f) EUV wave events (1)-(3) presenting the primary (blue curves) and reflected (red curves) wave fronts. (f) Yellow meridians define the 45° sector used for the analysis of the reflected wave kinematics. (axes in arcsec)

only 2 hours. SWAP takes images at a wavelength of 174 Å (cadence: $\sim$ 85 s), which is comparable to the EUVI 171 Å passband. To compare the observations from ST-A and SWAP, all images were re-scaled to Earth distance. The EUVI 195 Å filtergrams were reduced using the SECCHI_prep routines available within SolarSoft. The SWAP data were prepped using the tools provided by the PROBA2 software team. For each wave event we differentially rotated the images to the same reference time. To emphasize the signature of the transient waves we created running ratio (RR) images, dividing each frame by a frame taken 10 minutes earlier, as well as base ratio (BR) images, where we divide each frame by a base image taken 20 minutes after the end of the event before. Additionally we applied a median filter over 5 pixels to each image to increase the visibility of large-scale structures like EUV waves and smooth out small-scale fluctuations.

3. Results

3.1. General wave characteristics

The three large-scale EUVI waves under study were launched from active region (AR) NOAA 11149 on January 27, 2011 within a period of 12 hours and were all reflected from the same coronal hole at the southern polar region. Each wave launch coincided with a GOES class B/C flare, and the associated coronal mass ejections (CMEs) with plane-of-sky speeds of $455\,\mathrm{km\,s^{-1}}$, $413\,\mathrm{km\,s^{-1}}$ and $416\,\mathrm{km\,s^{-1}}$, respectively, were coming into the LASCO C2 field-of-view (http://spaceweather.gmu.edu/seeds/lasco.php) at 11:00 UT, 12:48 UT, and 20:36 UT, respectively. ST-A observed the EUV waves on the solar disk with their ejection centers and the sites of the associated flares at the south-western edge of the AR (N30E15 at onset of the first wave). Note that the positions of the waves' onset centers were almost identic, taking the solar rotation into account. Due to the quadrature configuration of ST-A and SWAP the waves were recorded exactly on the limb by SWAP (Figure 1 (a) and (b)).

Generally the waves are best observed in the 195 Å channel of ST-A, peaking at $T \sim 1.4$ MK (Wills-Davey and Thompson, 1999), nevertheless they are also well visible in the SWAP 174 Å passband with a peak temperature of $T \sim 1$ MK. Movies 1 and 2 show ST-A and SWAP sequences of direct and RR full disk images, respectively, covering the full observation period. Unfortunately, since the PROBA2 spacecraft has to undergo Earth eclipses during this period of the year, there are data gaps during each event under study. Therefore we do not have full data coverage in the limb observations, but in each case the onset of the wave as well as the entire phase of the wave reflection was recorded.

All three waves propagate in the same direction and show an angular extent of $\sim 120°$. As the wave fronts also have similar appearance these large-scale EUV waves can be considered as homologous (c. f. Kienreich *et al.*, 2011). Their similarity is evident in Figure 1(d)-(f), where for each wave event a ST-A RR image together with all tracked wave fronts is plotted. Primary wave fronts are displayed in blue, reflected waves are shown in red. The yellow dash-dotted contours outline the border of the southern coronal hole (S-CH), where each wave was reflected. We note that the main propagation directions of the primary and reflected waves are at an angle of $\sim 20°$ to each other, which obeys the laws of reflection.

3.2. Primary Waves

Figure 2 shows the evolution of the second wave in simultaneous RR snapshots from ST-A and SWAP, extracted from movies 1 and 2. In movie 1 we observed the onset of a rising loop system at ∼11:50 UT, before the first wave front appeared at 12:00 UT. The primary EUV wave traveling southward could be followed in the movies until 12:45 UT. Yet, the last wave front, we could manually track with reasonable certainty, was recorded at 12:40 UT. The first two panels in each column of Figure 2 illustrate the early phase of the primary wave, starting five minutes after the first wave front was observed. While the wave fronts

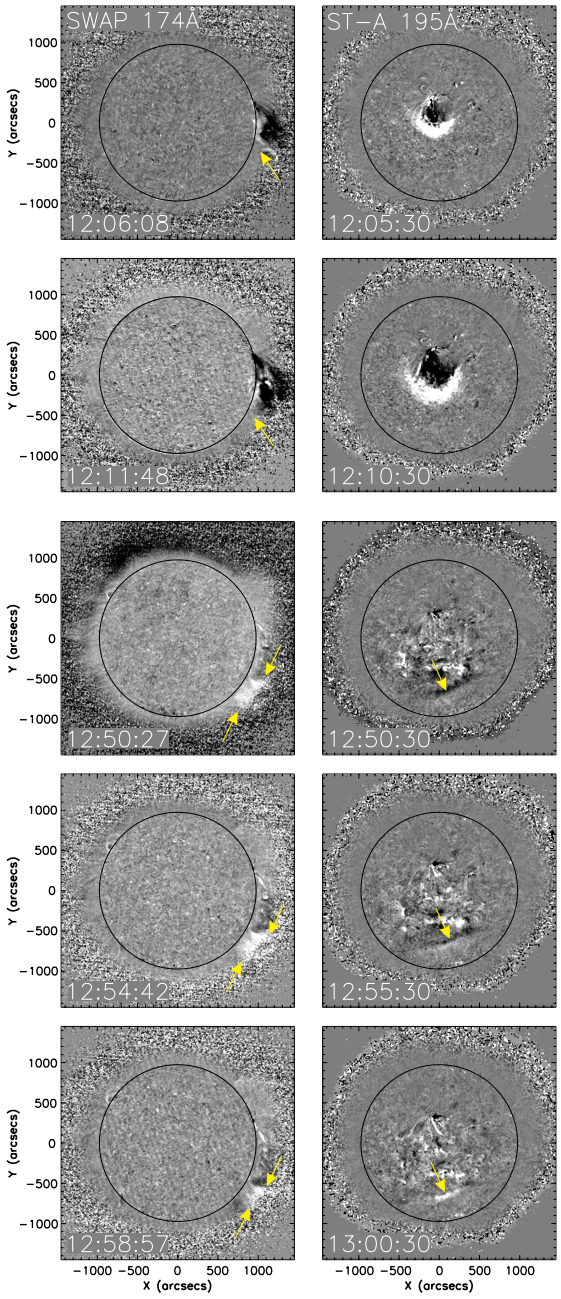

Figure 2. Sequence of median-filtered running ratio images of EUV wave event 2 recorded in the plane-of-sky in the SWAP 174Å (left) and on-disk in the EUVI 195Å channel (right). The first two panels show the early evolution of the primary wave, marked by yellow arrows in PROBA2. The last three panels display the evolution of the reflected wave. Yellow arrows in the ST-A images point to the front of the reflected wave. In contemporaneous SWAP frames the lateral width of the projected wave is indicated by two arrows. (See also movie 1 (ST-A) and movie 2 (PROBA2).)

are clearly discernible in the 195 Å ST-A images, they are rather faint in the SWAP recordings (Figure 2(left); yellow arrows). The SWAP images also show the erupting CME structure, which is highly asymmetric, pointing strongly to the South. The last three images per column display the evolution of the reflected wave and will be discussed in section 3.3.

The determination of the wave front distances is based on the visual tracking method, applied to the series of ST-A RR images. For the study of the wave kinematics we analyzed each of the three wave events individually. Moreover, the primary and the reflected wave of each event were investigated separately. As we are particularly interested in the wave reflection, we concentrated on subsections of the wave fronts propagating towards the S-CH (Figure 1(b)-(f); yellow dash-dotted line). Hence, we took only those parts of the fronts into account, which lay inside a chosen 45° sector pointing exactly to the South. This sector is indicated by the red meridians in Figure 1(c). The intersection point of the two red lines is the onset center of the wave, which was derived by employing circular fits to the first two tracked wave fronts. This calculation as well as the determination of the wave front distances from the wave center is carried out in 3D spherical coordinates, for details we refer to Veronig *et al.* (2006).

Figure 3 shows the time distance diagrams of all three wave events with superimposed error bars. The dash-dotted line at ~ 950 Mm outlines the mean distance of the S-CH border. In the case of the third event a wave front was already detected at 20:05 UT. Although, as in the RR-image the wave signature could not be fully disentangled from the signature of the emerging loop structure, we excluded the corresponding distance value. Taking this uncertainty into account, in all three cases the observation of the first wave front coincides with the peak time of the associated GOES class B/C flares (see also movie 1). Figure 3 (b) also shows that a metric type II radio burst was recorded during event 2 starting at 12:08 UT and ending at 12:27 UT. The two Radio Solar Telescope Network (RSTN; ftp://ftp.ngdc.noaa.gov/STP/SOLAR_DATA/SOLAR_RADIO/) stations San Vito (Brindisi, Italy, 18E 41N) and Palehua (Oahu, HI, 158W 21N), which observed the type II burst, estimated shock speeds of $900\,\mathrm{km\,s^{-1}}$ (San Vito) and $730\,\mathrm{km\,s^{-1}}$ (Palehua), respectively.

For each event we applied linear as well as least-square quadratic fits to the kinematical curves of the primary wave. Additionally the 95% confidence interval (Figure 4; grey areas) and the prediction interval were calculated for the linear fit. This gives us a means to decide whether the linear or the quadratic function better represents the wave kinematics. For wave 2 the velocities, gained with the two fitting methods, differ strongly. The linear fit gives a mean wave velocity of $314 \pm 16\,\mathrm{km\,s^{-1}}$, while the quadratic fit yields a velocity of $502 \pm 56\,\mathrm{km\,s^{-1}}$ at the first observed wave front and a constant deceleration of $106 \pm 29\,\mathrm{m\,s^{-2}}$. The derived velocities of wave 1 are smaller with $216 \pm 13\,\mathrm{km\,s^{-1}}$ resulting from the linear fit and $355 \pm 34\,\mathrm{km\,s^{-1}}$ (at the first observed front) from the quadratic fit with a constant deceleration of $65 \pm 17\,\mathrm{m\,s^{-2}}$. Wave 1 and 2, both show a distinct deceleration, in accordance with previous studies of large-scale EUV waves (e.g. Veronig, Temmer, and Vršnak, 2008; Long *et al.*, 2008; Grechnev *et al.*, 2011). However, wave 3 shows a different kinematic, as both fits indicate propagation with constant velocity of $\sim 270 \pm 11\,\mathrm{km\,s^{-1}}$ (linear)

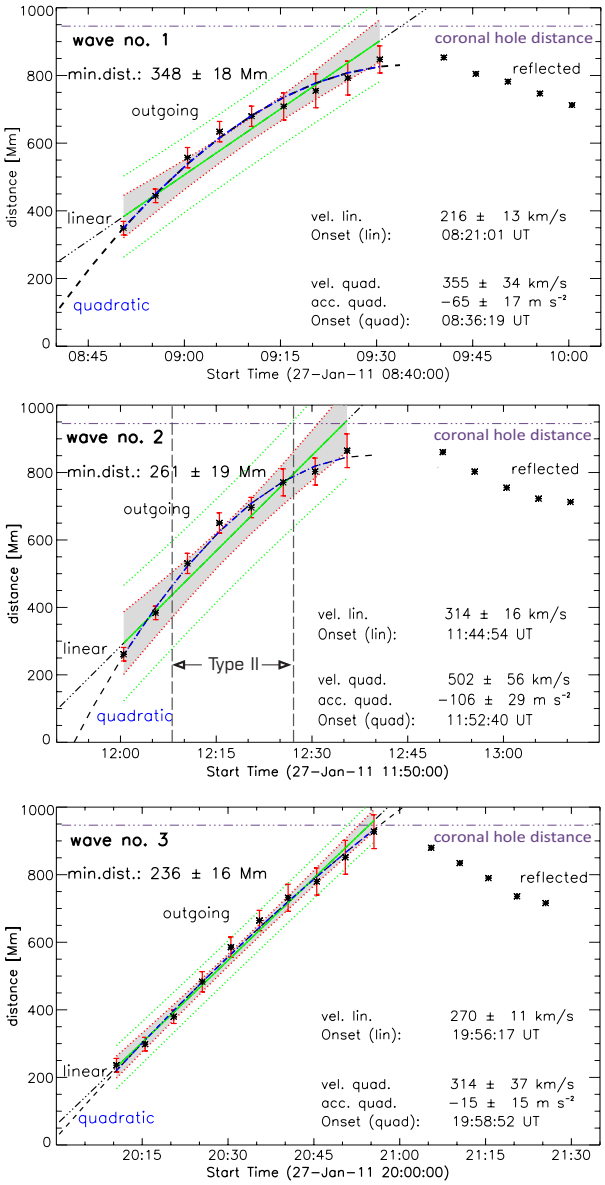

Figure 3. Kinematics of primary waves plus error bars reflecting the diffusiveness of the wave fronts. The distances from the wave onset center were derived for a 45° sector (cf. Fig. 1(c); pink star and red meridians). The distances of the reflected wave fronts with respect to the same center and sector are also shown. A linear (green) and a quadratic (blue) least square fit to the primary wave data are overlaid. The grey area indicates the 95% confidence interval of the linear fit. The dash dotted line in each diagram denotes the average distance of the coronal hole boundary. The velocities derived from the 2nd order polynomial fit are specified for the first observed wave front. (b) During event 2 also a type II burst (12:08-12:27 UT; grey dashed lines) was recorded by the Radio Solar Telescope Network observatories San Vito and Palehua.

and $314 \pm 37\,\mathrm{km\,s^{-1}}$ (quadratic), respectively. The quadratic fit suggests a small deceleration of $\sim 15 \pm 15\,\mathrm{m\,s^{-2}}$. Observations of EUV waves moving at constant speed were already reported by Ma *et al.* (2009), Kienreich, Temmer, and Veronig (2009).

3.3. Reflected Waves and lateral view of the events

In Movie 3 we show a sequence of ST-A RR and direct images, giving a close view of the area, in which the reflected wave 2 was observed best. Although faint, the reflected wave can even be detected in the original ST-A images. In Figure 2 the last three panels illustrate the propagation of the reflected wave 2. It was seen first at 12:50 UT and could be followed until 13:10 UT. The on-disk signatures of the reflected waves, marked by yellow arrows, have an inclination of $\sim 20^\circ$ with respect to ST-A's north-south axis. In the lateral view of SWAP we recognize a bright feature at and above the limb with an initial angular extent of $\sim 25^\circ$ (12:50 UT). The narrow configuration forming its northern edge did not change its position with time. At closer inspection it revealed itself as one root of a loop connecting to the CME ejection center. The broad southern part, which we assume to be the plane-of-sky signature of the EUV wave, moved northward approaching the inanimate loop. In the end, the angular extent of the bright feature had decreased to $\lesssim 10^\circ$ (13:10 UT). This motion clearly mirrors the northward directed propagation of the reflected EUV wave as seen by ST-A.

The derivation of the kinematics for the reflected waves followed the same pattern as previously described for the primary waves. To accurately determine their distances, particularly taking the altered propagation direction into account, we chose a new reference point at the border of the coronal hole and took a different 45° sector pointing to the northeast with an inclination of 20° relative to the solar north-south axis. The new sector of interest is depicted as yellow meridians in Figure 1(f).

Figure 4 shows the wave kinematics of all three reflected waves. Again error bars, the 95% confidence interval and the prediction interval are overlaid. We applied linear and least-square quadratic fits to the data. In all three cases we derived a deceleration; however, for wave 1 a constant propagation is also conceivable taking into account the error bars. Contrary to the primary waves, where we found wave 2 to be the fasted and wave 3 the slowest event, reflected wave 3 has the highest start velocity with $233 \pm 90\,\mathrm{km\,s^{-1}}$ and a deceleration of $63\,\mathrm{m\,s^{-2}}$. Wave 2 and wave 1 have start velocities of $192 \pm 89\,\mathrm{km\,s^{-1}}$ and $130 \pm 85\,\mathrm{km\,s^{-1}}$, respectively, and experience a constant deceleration of $45\,\mathrm{m\,s^{-2}}$ (wave 2) and $25\,\mathrm{m\,s^{-2}}$ (wave 1). We speculate that the reason for the higher start velocity of reflected wave 3 lies in the fact that its related primary wave is barely decelerated and hence has not dissipated much of its initial energy. Wave 1 and wave 2, on the other hand, experienced a strong deceleration going along with a considerable loss of energy. Thus, at the time of the reflection at the boarder of the S-CH, the velocity of primary wave 3 is higher than that of primary wave 1 or primary wave 2.

In order to discern the reflected wave more clearly we created stack plots from slices cut out from ST-A RR and BR images. Each slice has a width of 14 pixels

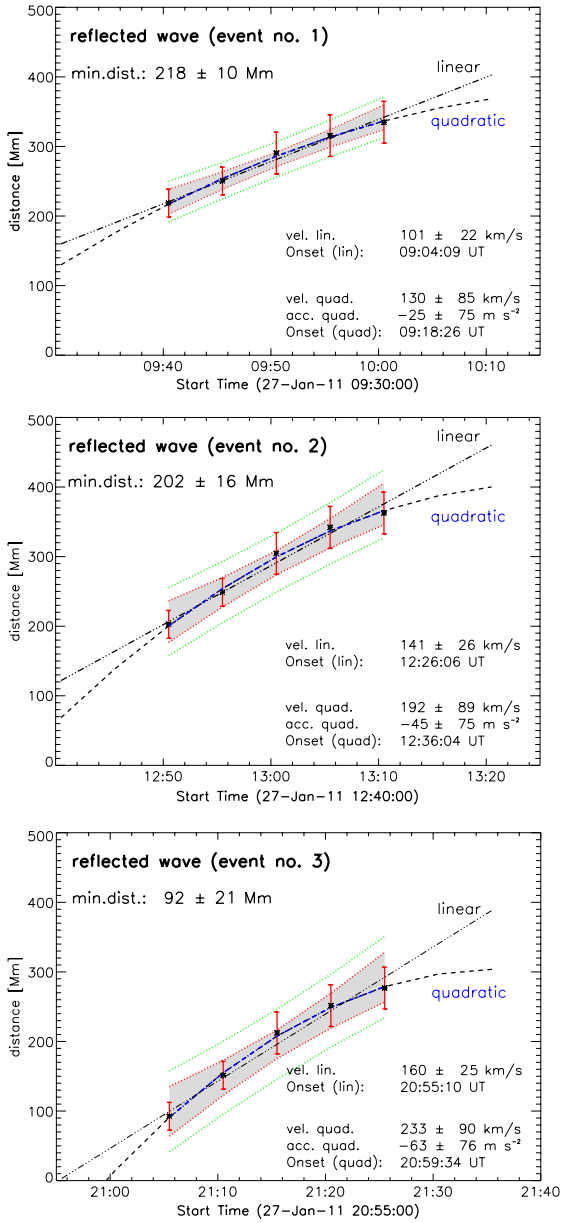

Figure 4. Time-distance diagrams of reflected waves together with linear and quadratic fits and error bars. Grey areas illustrate the 95% confidence bands for each linear fit. The kinematics of the reflected waves were derived using a reference point at the border of the coronal hole and a 45° sector (cf. Fig. 1(f), green star and yellow meridians), which represents the propagation direction of the reflected waves best.

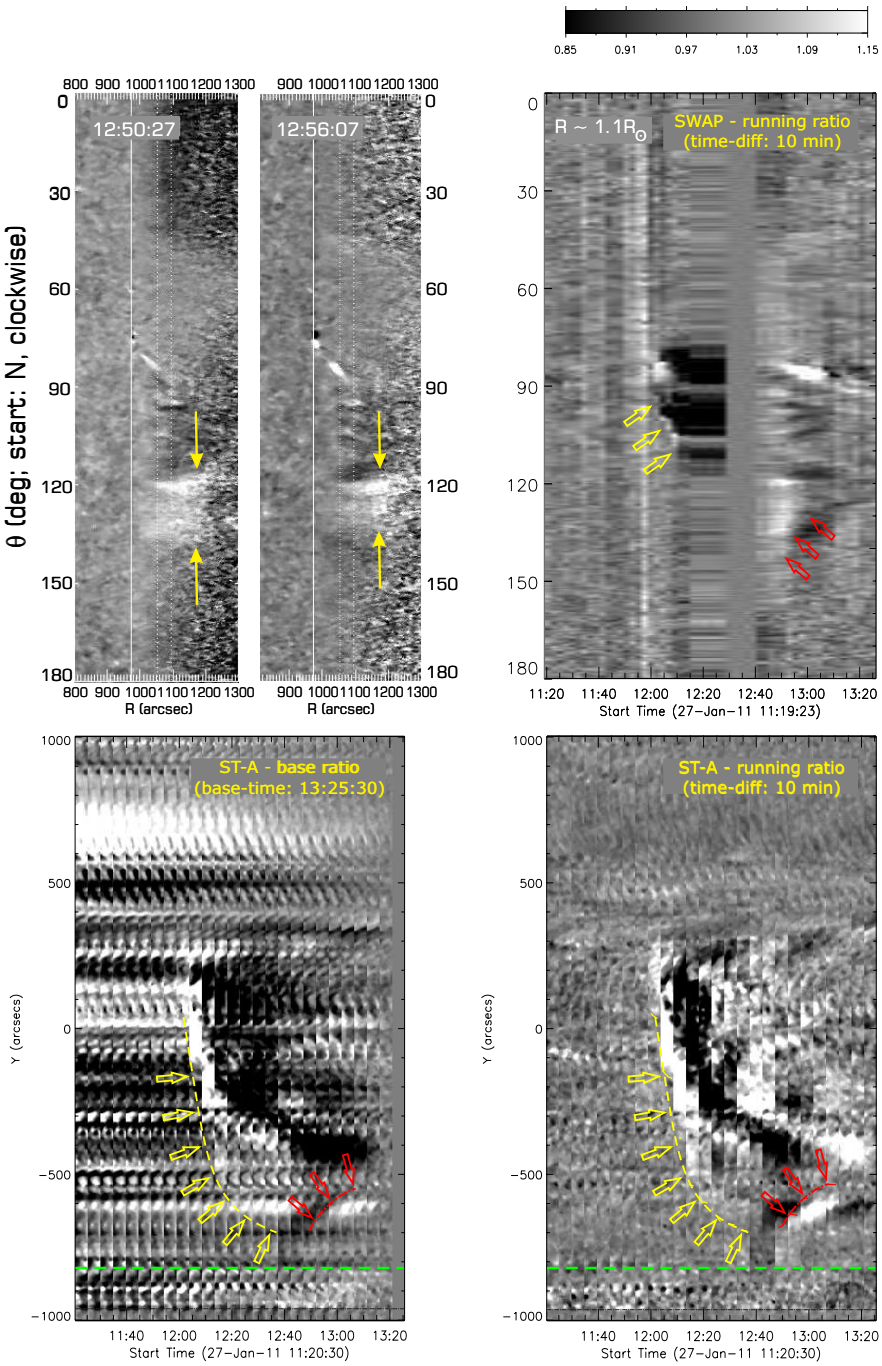

Figure 5. (a) Polar display of two PROBA2 RR-images taken in the plane-of-sky at $R = 800''$ to $1300''$; $\theta = 0°$ to $180°$ (c.f. Fig.1(a) yellow semi-circles). Slices along θ at a height of $\sim 100''$ were cut out. The resulting stack-plot for event 2 is given in (b). (d) On-disk stack-plot of ST-A 195Å RR-images. The wave propagation is outlined by the yellow curve (primary) and by the red curve (reflected). The green dashed line represents the border of the coronal hole. The reflected wave is also evident in the stack-plot of ST-A 195Å BR-images shown in panel (c).

and its vertical axis spans from $-1000''$ to $1000''$. The position and direction (20° to NS) of such rectangular slice is exhibited as blue rectangle in Figure 1(c). In the resulting stack plot for event 2 (Figure 5(d)) slices of RR images taken at subsequent time-indices are stacked together and reveal the evolution of wave 2 along the slit. The primary wave appears as a bright front moving downwards, and the reflected wave is a bright front running upwards. Both show a distinct deceleration which is mirrored by the yellow parabolic curve tracing the primary wave front and by the red 2^{nd} degree curve outlining the foremost part of the reflected wave. To confirm that the observed features, which we assume to be reflected waves, are not just artifacts in the RR images, where a previously dark feature shows itself as bright feature in the next frame and vice versa, we also generated stack plots from BR images, with the base image taken 20 minutes after the last observed reflected wave front. As it is obvious from Figure 5(c), the reflected wave is recognizable in the BR stack plot without any doubt, hence the feature is a real physical observable.

In the following we compare the ST-A on-disk stack plots with stack plots generated from the PROBA2 plane-of-sky images. For this purpose a semi-circular ring [$R = 800''$ to $1300''$ and $\theta = 0$ to 180° (starting at N and going clockwise)] was cut out from each PROBA2 RR image. In Figure 1(a) this area is marked by yellow semi-circles. As next step we transform this cut-out region, originally given in Cartesian (x,y)-coordinates, into polar (R, θ)-coordinates; two representative plots are displayed in Figure 5(a) with R (arcsec) along the horizontal and θ (degree) along the vertical axis. Finally slices at different coronal heights are cut out and stacked together. The resulting plot for a height of $H \sim 0.1\,R_\odot$ is shown in Figure 5(b). At the onset of the event the primary wave appears as a bright feature moving to larger θ–values (Figure 5(b) yellow arrows). Between 12:15 UT and 12:40 UT we do not have records from the wave commencement, as PROBA2 experienced an eclipse during this time, but SWAP observed the entire propagation of the reflected wave (Figure 5(b) red arrows). It is obvious from Figure 5(b) and (d) that the bright feature moving upwards in the ST-A on-disk slice coincides with the bright structure proceeding to smaller θ–values in the SWAP plane-of-sky slice. We can conclude that the same coronal EUV wave is simultaneously observed in quadrature by both instruments.

In Figure 6 we show four stack plots extracted from slices centered at $0''$(limb), $50''(\sim 0.05\,R_\odot), 100''(\sim 0.1\,R_\odot)$ and $150''(\sim 0.15\,R_\odot)$ above the limb. These plots reveal that the strongest signatures of the primary wave and reflected wave move at different heights. While the primary wave is brightest at the limb up to $R \sim 1.05\,R_\odot$, it is merely recognizable at $1.1\,R_\odot$ and imperceptible at $1.15\,R_\odot$. The signature of the reflected wave however is strongest in a radial distance range of $R = 1.1$ to $1.15\,R_\odot$, the strength of the wave signal decreases to larger as well as to smaller heights. At $1.05\,R_\odot$ the wave signature is very faint and at the limb there is no evidence of the wave at all. These findings suggest that the waves were not simply reflected in a two-dimensional plane at a fixed height, but that they were also reflected to larger coronal heights.

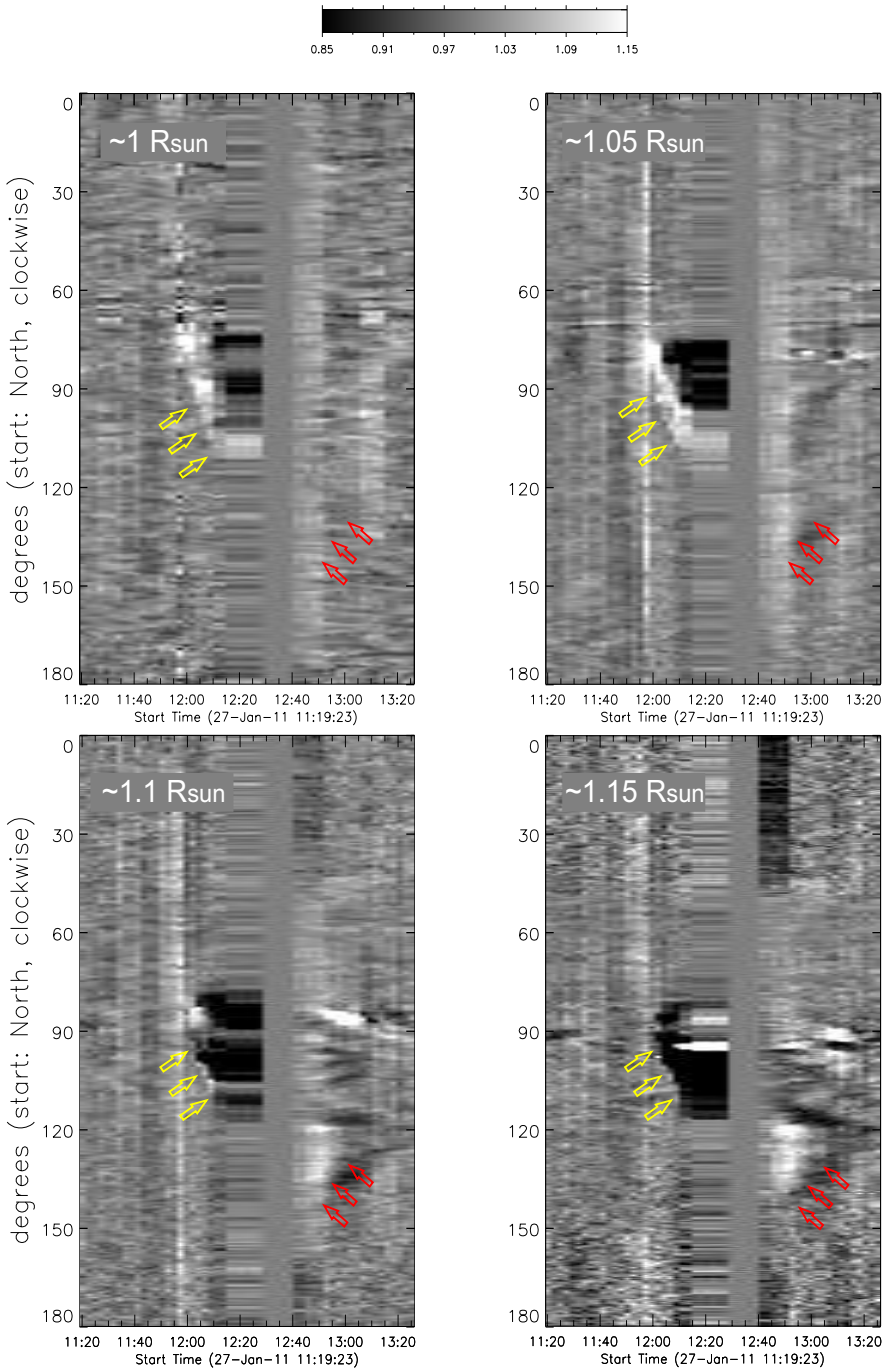

Figure 6. PROBA2 RR-stack plots for different heights above the solar limb (cf. Fig. 5(a)). The signature of the primary wave (yellow arrows) is evident at $R \sim 1\,R_{\odot}$ (a) and $R \sim 1.05 R_{\odot}$ (b). It is barely visible at larger heights, as shown in (c) and (d). The data gap in all four plots between 12:15 UT and 12:40 UT is due to a PROBA2 eclipse. The reflected waves (red arrows) show the strongest signature in a height range of $H \sim 0.1$ to $0.15\,R_{\odot}$,(c) and (d), while they are invisible at the solar limb. Red arrows in panel (a) indicate the wave position at $H \sim 0.1 R_{\odot}$.

4. Discussion and Conclusion

We have presented observations of three homologous coronal EUV wave events in quadrature, recorded simultaneously in high cadence by ST-A and PROBA2 within a period of 12 hours. The on-disk view of ST-A revealed that all three primary large-scale EUV waves were ejected from the same onset center and showed a similar appearance and angular extent as well as the same propagation direction, and most important that they were all reflected from the same S-CH. PROBA2 delivered a lateral view of the events, showing the southward directed movement of the primary waves along the limb in a height range between 0 (limb) and $\sim 0.05\,R_{\odot}$ above the limb. Additional findings are: (1) EUV wave 1 and 2 with initial velocities of $\sim 350\,\mathrm{km\,s^{-1}}$ and $\sim 500\,\mathrm{km\,s^{-1}}$, respectively, showed a distinct deceleration, while wave 3 propagated at a constant speed of $\sim 270\,\mathrm{km\,s^{-1}}$. Their behavior and appearance strongly resembles the homologous events reported by Kienreich *et al.* (2011). (2) The fastest and strongest primary large-scale wave event 2 was accompanied by a metric type II burst indicative of a coronal shock wave. (3) Examination of the associated CMEs in the PROBA2 plane-of-sky view revealed a highly asymmetric shape, which was strongly bent to the south. This distorted expansion of the CME appears to be the reason for the nonuniform propagation of the large-scale EUV waves, which are most prominent in the south direction.

The primary focus of this paper, however, lies on the analysis of the three coronal wave events experiencing reflections at the boundary of a coronal hole. The CH-boundary did not change noticeably within the 12 hours period. Hence, as the primary waves are homologous, we expected the reflected waves also to be homologous. In the ST-A images it was indeed obvious that all three reflected waves had the same shape and propagated into the same direction $\sim 20^{\circ}$ inclined to the direction of the primary waves. This gives clear evidence that each primary and subsequently observed reflected wave belonged to the same event. The additional lateral view from PROBA2 revealed a northward directed motion at a height of ~ 0.1 to $0.15\,R_{\odot}$ fitting to the on-disk results. Our analysis of the reflected waves showed that the velocities in the range of $130\,\mathrm{km\,s^{-1}}$ to $230\,\mathrm{km\,s^{-1}}$ were smaller than those of their primary pendants. This can be attributed to the individual deceleration of the primary waves and explains why reflected wave 3 is now the fastest one with $\sim 230\,\mathrm{km\,s^{-1}}$. The results of our kinematical analysis were confirmed by our studies of the ST-A and PROBA2 stack-plots showing the same wave evolution along a chosen direction and height, respectively.

Yet, the most important result in our study is that this reflection process is also clearly evident in the base ratio images. These findings are in contrast to the interpretation of Attrill (2010), who assumed the reflected waves to be just artifacts of running ratio images. Our results are in good agreement with the conclusions from Gopalswamy *et al.* (2009) for the event on May 19, 2007. Like in our case, the reflected waves were slower than the primary wave, and the stack-plot for the eastward reflected wave showed a comparable evolution of the primary and reflected wave.

Our results – the homologous appearance of primary as well as reflected waves, their kinematics, and the type II burst during event 2 – strongly support our

assumption that the three observed EUV transients are fast-mode magnetosonic waves following the interpretations by Uchida.

Acknowledgements I.W.K., N.M., and A.M.V. acknowledge the Austrian Science Fund (FWF): P20867-N16. The MOEL Förderungsprogramm is acknowledged by N.M. The European Community's Seventh Framework Programme (FP7/ 2007-2013) under grant agreement no. 218816 (SOTERIA) is acknowledged (B.V., M.T.). We thank the PROBA2 team and STEREO/SECCHI teams for their open data policy. I.W.K. thanks the PROBA2 team members for their support during her stay at the Royal Observatory of Belgium as PROBA2 guest investigator.

References

Attrill, G.D.R.: 2010, Dispelling Illusions of Reflection: A New Analysis of the 2007 May 19 Coronal "Wave" Event. *Astrophys. J.* **718**, 494 – 501. doi:10.1088/0004-637X/718/1/494.

Attrill, G.D.R., Harra, L.K., van Driel-Gesztelyi, L., Démoulin, P.: 2007, Coronal "Wave": Magnetic Footprint of a Coronal Mass Ejection? *Astrophys. J. Lett.* **656**, 101 – 104. doi:10.1086/512854.

Berghmans, D., Hochedez, J.F., Defise, J.M., Lecat, J.H., Nicula, B., Slemzin, V., Lawrence, G., Katsyiannis, A.C., van der Linden, R., Zhukov, A., Clette, F., Rochus, P., Mazy, E., Thibert, T., Nicolosi, P., Pelizzo, M.-G., Schühle, U.: 2006, SWAP onboard PROBA 2, a new EUV imager for solar monitoring. *Advances in Space Research* **38**, 1807 – 1811. doi:10.1016/j.asr.2005.03.070.

Biesecker, D.A., Myers, D.C., Thompson, B.J., Hammer, D.M., Vourlidas, A.: 2002, Solar Phenomena Associated with "EIT Waves". *Astrophys. J.* **569**, 1009 – 1015. doi:10.1086/339402.

Chen, P.F., Fang, C.: 2005, EIT waves – A signature of global magnetic restructuring in CMEs. In: Dere, K., Wang, J., Yan, Y. (eds.) *Coronal and Stellar Mass Ejections*, *IAU Symposium* **226**, 55 – 64. doi:10.1017/S1743921305000141.

Chen, P.F., Wu, S.T., Shibata, K., Fang, C.: 2002, Evidence of EIT and Moreton Waves in Numerical Simulations. *Astrophys. J. Lett.* **572**, 99 – 102. doi:10.1086/341486.

Cohen, O., Attrill, G.D.R., Manchester, W.B. IV, Wills-Davey, M.J.: 2009, Numerical Simulation of an EUV Coronal Wave Based on the February 13, 2009 CME Event Observed by STEREO. *ArXiv e-prints*.

Dai, Y., Auchère, F., Vial, J., Tang, Y.H., Zong, W.G.: 2010, Large-scale Extreme-Ultraviolet Disturbances Associated with a Limb Coronal Mass Ejection. *Astrophys. J.* **708**, 913 – 919. doi:10.1088/0004-637X/708/2/913.

Delannée, C., Aulanier, G.: 1999, Cme Associated with Transequatorial Loops and a Bald Patch Flare. *Solar Phys.* **190**, 107 – 129. doi:10.1023/A:1005249416605.

Gallagher, P.T., Long, D.M.: 2010, Large-scale Bright Fronts in the Solar Corona: A Review of "EIT waves". *Space Sci. Rev.*, 127 – . doi:10.1007/s11214-010-9710-7.

Gopalswamy, N., Yashiro, S., Temmer, M., Davila, J., Thompson, W.T., Jones, S., McAteer, R.T.J., Wuelser, J.-P., Freeland, S., Howard, R.A.: 2009, EUV Wave Reflection from a Coronal Hole. *Astrophys. J. Lett.* **691**, 123 – 127. doi:10.1088/0004-637X/691/2/L123.

Grechnev, V.V., Afanasyev, A.N., Uralov, A.M., Chertok, I.M., Eselevich, M.V., Eselevich, V.G., Rudenko, G.V., Kubo, Y.: 2011, Coronal Shock Waves, EUV Waves, and Their Relation to CMEs. III. Shock-Associated CME/EUV Wave in an Event with a Two-Component EUV Transient. *ArXiv e-prints*.

Halain, J.-P., Berghmans, D., Defise, J.-M., Renotte, E., Thibert, T., Mazy, E., Rochus, P., Nicula, B., de Groof, A., Seaton, D., Schühle, U.: 2010, First light of SWAP on-board PROBA2. In: *Society of Photo-Optical Instrumentation Engineers (SPIE) Conference Series*, *Presented at the Society of Photo-Optical Instrumentation Engineers (SPIE) Conference* **7732**. doi:10.1117/12.857979.

Howard, R.A., Moses, J.D., Vourlidas, A., Newmark, J.S., Socker, D.G., Plunkett, S.P., Korendyke, C.M., Cook, J.W., Hurley, A., Davila, J.M., Thompson, W.T., St Cyr, O.C., Mentzell, E., Mehalick, K., Lemen, J.R., Wuelser, J.P., Duncan, D.W., Tarbell, T.D., Wolfson, C.J., Moore, A., Harrison, R.A., Waltham, N.R., Lang, J., Davis, C.J., Eyles, C.J., Mapson-Menard, H., Simnett, G.M., Halain, J.P., Defise, J.M., Mazy, E., Rochus, P., Mercier, R., Ravet, M.F., Delmotte, F., Auchere, F., Delaboudiniere, J.P., Bothmer, V., Deutsch, W., Wang, D., Rich, N., Cooper, S., Stephens, V., Maahs, G., Baugh, R., McMullin, D., Carter, T.: 2008, Sun Earth Connection Coronal and Heliospheric Investigation (SECCHI). *Space Science Reviews* **136**, 67 – 115. doi:10.1007/s11214-008-9341-4.

Hudson, H.S., Khan, J.I., Lemen, J.R., Nitta, N.V., Uchida, Y.: 2003, Soft X-ray observation of a large-scale coronal wave and its exciter. *Solar Phys.* **212**, 121 – 149. doi:10.1023/A:1022904125479.

Kaiser, M.L., Kucera, T.A., Davila, J.M., St. Cyr, O.C., Guhathakurta, M., Christian, E.: 2008, The STEREO Mission: An Introduction. *Space Science Reviews* **136**, 5 – 16. doi:10.1007/s11214-007-9277-0.

Khan, J.I., Aurass, H.: 2002, X-ray observations of a large-scale solar coronal shock wave. *Astron. Astrophys.* **383**, 1018 – 1031. doi:10.1051/0004-6361:20011707.

Kienreich, I.W., Temmer, M., Veronig, A.M.: 2009, STEREO Quadrature Observations of the Three-Dimensional Structure and Driver of a Global Coronal Wave. *Astrophys. J. Lett.* **703**, 118 – 122. doi:10.1088/0004-637X/703/2/L118.

Kienreich, I.W., Veronig, A.M., Muhr, N., Temmer, M., Vršnak, B., Nitta, N.: 2011, Case Study of Four Homologous Large-scale Coronal Waves Observed on 2010 April 28 and 29. *Astrophys. J. Lett.* **727**, L43+. doi:10.1088/2041-8205/727/2/L43.

Klassen, A., Aurass, H., Mann, G., Thompson, B.J.: 2000, Catalogue of the 1997 SOHO-EIT coronal transient waves and associated type II radio burst spectra. *Astron. Astrophys. Suppl.* **141**, 357 – 369. doi:10.1051/aas:2000125.

Liu, W., Nitta, N.V., Schrijver, C.J., Title, A.M., Tarbell, T.D.: 2010, First SDO AIA Observations of a Global Coronal EUV "Wave": Multiple Components and "Ripples". *Astrophys. J. Lett.* **723**, 53 – 59. doi:10.1088/2041-8205/723/1/L53.

Long, D.M., Gallagher, P.T., McAteer, R.T.J., Bloomfield, D.S.: 2008, The Kinematics of a Globally Propagating Disturbance in the Solar Corona. *Astrophys. J. Lett.* **680**, 81 – 84. doi:10.1086/589742.

Ma, S., Wills-Davey, M.J., Lin, J., Chen, P.F., Attrill, G.D.R., Chen, H., Zhao, S., Li, Q., Golub, L.: 2009, A New View of Coronal Waves from STEREO. *Astrophys. J.* **707**, 503 – 509. doi:10.1088/0004-637X/707/1/503.

Moses, D., Clette, F., Delaboudinière, J., Artzner, G.E., Bougnet, M., Brunaud, J., Carabetian, C., Gabriel, A.H., Hochedez, J.F., Millier, F., Song, X.Y., Au, B., Dere, K.P., Howard, R.A., Kreplin, R., Michels, D.J., Defise, J.M., Jamar, C., Rochus, P., Chauvineau, J.P., Marioge, J.P., Catura, R.C., Lemen, J.R., Shing, L., Stern, R.A., Gurman, J.B., Neupert, W.M., Newmark, J., Thompson, B., Maucherat, A., Portier-Fozzani, F., Berghmans, D., Cugnon, P., van Dessel, E.L., Gabryl, J.R.: 1997, EIT Observations of the Extreme Ultraviolet Sun. *Solar Phys.* **175**, 571 – 599. doi:10.1023/A:1004902913117.

Ofman, L., Thompson, B.J.: 2002, Interaction of EIT Waves with Coronal Active Regions. *Astrophys. J.* **574**, 440 – 452. doi:10.1086/340924.

Patsourakos, S., Vourlidas, A.: 2009, "Extreme Ultraviolet Waves" are Waves: First Quadrature Observations of an Extreme Ultraviolet Wave from STEREO. *Astrophys. J. Lett.* **700**, 182 – 186. doi:10.1088/0004-637X/700/2/L182.

Podladchikova, O., Berghmans, D.: 2005, Automated Detection Of Eit Waves And Dimmings. *Solar Phys.* **228**, 265 – 284. doi:10.1007/s11207-005-5373-z.

Temmer, M., Veronig, A.M., Gopalswamy, N., Yashiro, S.: 2011, Relation Between the 3D-Geometry of the Coronal Wave and Associated CME During the 26 April 2008 Event. *Solar Phys.*, 75 – . doi:10.1007/s11207-011-9746-1.

Thompson, B.J., Myers, D.C.: 2009, A Catalog of Coronal "EIT Wave" Transients. *Astrophys. J. Suppl.* **183**, 225 – 243. doi:10.1088/0067-0049/183/2/225.

Thompson, B.J., Plunkett, S.P., Gurman, J.B., Newmark, J.S., St. Cyr, O.C., Michels, D.J.: 1998, SOHO/EIT observations of an Earth-directed coronal mass ejection on May 12, 1997. *Geophys. Res. Lett.* **25**, 2465 – 2468. doi:10.1029/98GL50429.

Thompson, B.J., Gurman, J.B., Neupert, W.M., Newmark, J.S., Delaboudinière, J.-P., St. Cyr, O.C., Stezelberger, S., Dere, K.P., Howard, R.A., Michels, D.J.: 1999, SOHO/EIT Observations of the 1997 April 7 Coronal Transient: Possible Evidence of Coronal Moreton Waves. *Astrophys. J. Lett.* **517**, 151 – 154. doi:10.1086/312030.

Veronig, A.M., Temmer, M., Vršnak, B.: 2008, High-Cadence Observations of a Global Coronal Wave by STEREO EUVI. *Astrophys. J. Lett.* **681**, 113 – 116. doi:10.1086/590493.

Veronig, A.M., Temmer, M., Vršnak, B., Thalmann, J.K.: 2006, Interaction of a Moreton/EIT Wave and a Coronal Hole. *Astrophys. J.* **647**, 1466 – 1471. doi:10.1086/505456.

Veronig, A.M., Muhr, N., Kienreich, I.W., Temmer, M., Vršnak, B.: 2010, First Observations of a Dome-shaped Large-scale Coronal Extreme-ultraviolet Wave. *Astrophys. J. Lett.* **716**, 57 – 62. doi:10.1088/2041-8205/716/1/L57.

Vršnak, B., Warmuth, A., Temmer, M., Veronig, A., Magdalenić, J., Hillaris, A., Karlický, M.: 2006, Multi-wavelength study of coronal waves associated with the CME-flare event of 3 November 2003. *Astron. Astrophys.* **448**, 739 – 752. doi:10.1051/0004-6361:20053740.

Wang, Y.-M.: 2000, EIT Waves and Fast-Mode Propagation in the Solar Corona. *Astrophys. J. Lett.* **543**, 89 – 93. doi:10.1086/318178.

Warmuth, A.: 2010, Large-scale waves in the solar corona: The continuing debate. *Advances in Space Research* **45**, 527 – 536. doi:10.1016/j.asr.2009.08.022.

Warmuth, A., Vršnak, B., Aurass, H., Hanslmeier, A.: 2001, Evolution of Two EIT/Hα Moreton Waves. *Astrophys. J. Lett.* **560**, 105 – 109. doi:10.1086/324055.

White, S.M., Thompson, B.J.: 2005, High-Cadence Radio Observations of an EIT Wave. *Astrophys. J. Lett.* **620**, 63 – 66. doi:10.1086/428428.

Wills-Davey, M.J., Attrill, G.D.R.: 2010, EIT Waves: A Changing Understanding over a Solar Cycle. *Space Science Reviews*, 22 – . doi:10.1007/s11214-009-9612-8.

Wills-Davey, M.J., Thompson, B.J.: 1999, Observations of a Propagating Disturbance in TRACE. *Solar Phys.* **190**, 467 – 483. doi:10.1023/A:1005201500675.

Wills-Davey, M.J., DeForest, C.E., Stenflo, J.O.: 2007, Are "EIT Waves" Fast-Mode MHD Waves? *Astrophys. J.* **664**, 556 – 562. doi:10.1086/519013.

Zhukov, A.N.: 2011, EIT wave observations and modeling in the STEREO era. *Journal of Atmospheric and Solar-Terrestrial Physics* **73**, 1096 – 1116. doi:10.1016/j.jastp.2010.11.030.

Zhukov, A.N., Auchère, F.: 2004, On the nature of EIT waves, EUV dimmings and their link to CMEs. *Astron. Astrophys.* **427**, 705 – 716. doi:10.1051/0004-6361:20040351.